

# Calorimetric study on the decomposition of hydroxylamine in the presence of transition metals

Mieko Kumasaki\*

National Institute of Industrial Safety, 1-4-6 Umezono Kiyose, Tokyo 204-0024, Japan

Available online 7 August 2004

## Abstract

Hydroxylamine (HA), hydroxylamine chloride (HACl), and hydroxylamine nitrate (HAN) were each mixed with aqueous solutions of  $\text{Cr}^{3+}$ ,  $\text{Cr}^{6+}$ ,  $\text{Mn}^{7+}$ ,  $\text{Co}^{2+}$ ,  $\text{Co}^{3+}$ , and  $\text{Cu}^{2+}$ , and their heat flow profiles were monitored by a small-scaled reaction calorimeter, SuperCRC. These mixing tests demonstrated that HA was less reactive than HACl and HAN with  $\text{Mn}^{7+}$  and  $\text{Cr}^{6+}$ . Their UV–vis spectra confirmed that the substrates reacted when  $\text{Mn}^{7+}$  and  $\text{Cr}^{6+}$  were reduced. HA was more reactive with  $\text{Cu}^{2+}$  than HACl and HAN and exhibited the highest reactivity among the three substrates with regard to metals in the intermediate oxidation states:  $\text{Cr}^{3+}$ ,  $\text{Co}^{3+}$ , and  $\text{Co}^{2+}$ . During the reaction of HA and  $\text{Co}^{3+}$ , an induction period was observed. All exothermic reactions were accompanied by precipitation or a change in the UV–vis spectra.

© 2004 Elsevier B.V. All rights reserved.

*Keywords:* Hydroxylamine; Transition metals; SuperCRC

## 1. Introduction

In the field of material safety, a considerable amount of interest in hydroxylamine (HA) was generated as a result of two tragic accidents that occurred in United States and Japan [1–4]. HA has many properties; one of the most attractive of them, namely, its reactivity with metals, is also very dangerous.

The chemical structure of HA implies that HA interacts with transition metals. This is because HA includes a nitrogen atom and an oxygen atom, both of which donate their lone pairs to transition metals. The donation affects the strength of the bonds in HA and sometimes makes HA unstable. Furthermore, some transition metals work as oxidizers because they can have several oxidation states and transition between different states as well as oxidize reducing agents, such as HA. Therefore, it is essential to investigate the reactivity of HA with transition metals for safe handling.

In this study, the calorimetric behaviors of HA, hydroxylamine chloride (HACl), and hydroxylamine nitrate (HAN)

caused by the Fe(III) ion were studied, and Fe(III) was found to trigger an exothermic reaction, especially in HA [5]. The maximum heat flow reached 434 mW in HA, 46 mW in HACl, and 21 mW in HAN. In this report, the calorimetric behaviors caused by  $\text{Cr}^{3+}$ ,  $\text{Cr}^{6+}$ ,  $\text{Mn}^{7+}$ ,  $\text{Co}^{2+}$ ,  $\text{Co}^{3+}$ , and  $\text{Cu}^{2+}$  are presented. They are in the highest or intermediate oxidation states, which allows them to act as oxidizers. The calorimetric behaviors were monitored using a small-scaled reaction calorimeter, SuperCRC, as described in a previous report [5]. Moreover, UV–vis absorption spectra were collected before and after the reactions in order to follow the redox reactions.

## 2 Experiments

### 2.1. Samples

For calorimetric measurements, an aqueous solution of HA and its salts were used. HA (MW 33.03) was purchased from the Aldrich as a 50 wt.% aq. solution, and HACl (MW 69.49) in the solid state was purchased from Wako Chemical, Japan. Two mol/l of HA and HACl was carefully prepared in deionized distilled water. Two moles/litre of HAN

\* Tel.: +81 424 91 4512; fax: +81 424 91 7846.

E-mail address: miggy@anken.go.jp (M. Kumasaki).

(MW 96.04) was obtained from Hosoya Pyrotechnics Co. Ltd., Japan.

Solutions of the transition metals were prepared in deionized distilled water to give 0.2 mmol/g of solutions by dissolving  $\text{Cr}(\text{NH}_4)(\text{SO}_4)_2 \cdot 12\text{H}_2\text{O}$  ( $\text{Cr}^{3+}$ , FW 478.34),  $\text{K}_2\text{Cr}_2\text{O}_7$  ( $\text{Cr}^{6+}$ , FW 294.18),  $\text{KMnO}_7$  ( $\text{Mn}^{7+}$ , FW 158.03),  $\text{Co}(\text{NH}_4)_2(\text{SO}_4)_2 \cdot 6\text{H}_2\text{O}$  ( $\text{Co}^{2+}$ , FW 395.23),  $[\text{Co}(\text{NH}_4)_6]\text{Cl}_3$  ( $\text{Co}^{3+}$ , FW 267.47), and  $\text{Cu}(\text{NH}_4)_2(\text{SO}_4) \cdot 6\text{H}_2\text{O}$  ( $\text{Cu}^{2+}$ , FW 399.84). All the transition metal compounds were purchased from Wako Chemical, Japan.

### 1.2. SuperCRC

SuperCRC is a reaction calorimeter requiring less than 16 ml of sample. Its features were described in a previous report [5]. All experiments used 1 ml of HA water solutions and water and 0.1 g of metal ion solution.

HA aqueous solutions and 1 ml of water as a reference were placed in the calorimeter heat sink. The calorimeter block maintained the temperature at 25 °C. A magnetic stirrer provided continuous agitation in the substrate and reference. After the heat flow behavior was stabilized, the metal ion solutions were injected into each side through teflon tubes. Peltier devices built into the calorimeter heat sink detected the heat flow behavior that accompanied the reactions. Three trials were carried out for each sample, and the average values of the peak and overall heat of the reaction were calculated. A heat flow datum point was obtained every 3 s. The maximum test duration was 12.5 h, which was limited by the maximum of 15,000 points.

Before the reactions were observed, the heat absorptions caused by the  $\text{H}_2\text{O}$  injection were measured for HACl and HAN. The heat of dissolution was  $-0.61$  J for HAN, which was caused by the heat of dilution. HACl did not exhibit a change in heat flow. With regard to HA,  $-1.53$  J of the heat of dissolution was quoted from a previous report [5]. Concerning HAN, the overall heat of the reaction was calculated by subtracting this value to compensate for the dissolution.

### 1.3. UV-vis absorption spectrum

UV-vis absorption spectra in the range of 190–800 nm were collected using a Hitachi U-3310 spectrometer. The sample cells were quartz with a 10 mm path length. The sample and reference solutions were used for the SuperCRC measurements. All UV-vis spectra were background-substituted from a reference sample of water. The data were collected for the aqueous solutions of metals and liquid mixtures. When there was precipitation, the precipitates were so fine that they produced the Tyndall phenomenon, or light scattering. As a result, the collection of spectra was inhibited.

An absorption peak due to  $\text{NO}_3^-$ , which was observed at 300 nm in HAN, was omitted from the results in the present report.

## 2. Results and discussion

### 2.1. Reactions with $\text{Cr}^{3+}$ and $\text{Cr}^{6+}$

$\text{Cr}^{6+}$  has the highest oxidation state of any chromium and is a strong oxidizing reagent. On the other hand,  $\text{Cr}^{3+}$  has a lower oxidation state and is less oxidizing. The redox reactions can be investigated by comparing these two oxidative states, of chromium.

The heat flow profiles of the reactions with  $\text{Cr}^{3+}$  are shown in Fig. 1. Since the heat flow must include such processes as the heat of reactions, gas evolutions, dilution of substrates, and dissolution of hydrophilic gases, the calorimetric data represented the overall heat of the reactions. Table 1 summarizes the results of the calorimetric measurements and UV-vis spectra. In the table,  $\text{H}_2\text{O}$  as a substrate indicates the data from the aqueous solution of the metal ion.

No heat release was observed for HACl and HAN. Although the heat flow of HAN clearly showed heat absorption, the amount of heat absorbed was corrected by considering  $-0.61$  J as the heat of dilution. Since, the UV-vis spectra exhibited absorptions of  $\text{Cr}^{3+}$ , it was suggested that  $\text{Cr}^{3+}$  existed as  $[\text{Cr}(\text{H}_2\text{O})_6]^{3+}$ . No redox reaction occurred for the reductive HACl and HAN.

HA exothermically reacted with  $\text{Cr}^{3+}$ . The reaction produced a sage-green precipitate, and the precipitation color changed to violet in a few hours. The sage-green precipitation was  $\text{Cr}(\text{OH})_3$ , which is generated in an alkaline solution [6]. However, the generation mechanisms of the violet precipitate and the redox reactions are currently not understood.

Fig. 2 shows the exothermic behavior caused by  $\text{Cr}^{6+}$ . Table 2 is a summary of the experimental results. The reactions of HACl and HAN were completed within 30 min. When in contact with  $\text{CrO}_4^{2-}$ , HACl and HAN produced bubbles, and the yellow  $\text{CrO}_4^{2-}$  changed to a champagne color. The absorptions of  $\text{CrO}_4^{2-}$  disappeared, and new peaks appeared, suggesting the presence of  $[\text{Cr}(\text{H}_2\text{O})_6]^{3+}$ .

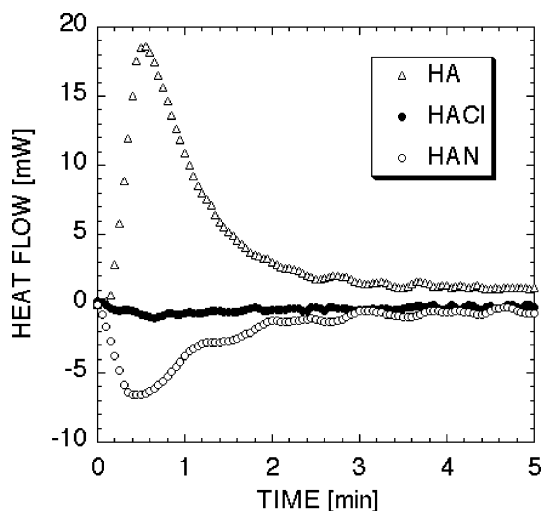


Fig. 1. Reaction heat flow as a function of time caused by  $\text{Cr}^{3+}$ .

Table 1  
Summary of the calorimetric and UV data of the reaction caused by  $\text{Cr}^{3+}$  (calorimetric values are the average of three trials)

Substrate	Maximum heat flow (Mw)	Overall heat of reaction (J)	Distinguishable peaks of UV absorptions (nm)	Color of reaction mixtures or precipitates
HA	17.7	2.47	Precipitation	Green sage > violet
HACl	-0.9	-0.19	422.0, 579.5	Dark purple
HAN	-9.9	-0.11	408.5, 580.5	Dark purple
H <sub>2</sub> O			425.5, 582.5	Dark purple

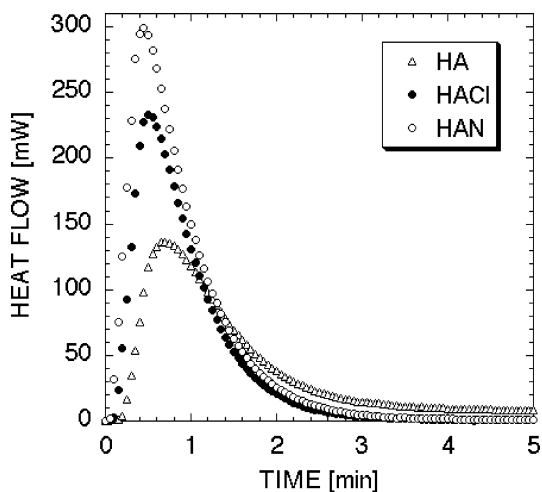


Fig. 2. Reaction heat flow as a function of time caused by  $\text{Cr}^{6+}$ .

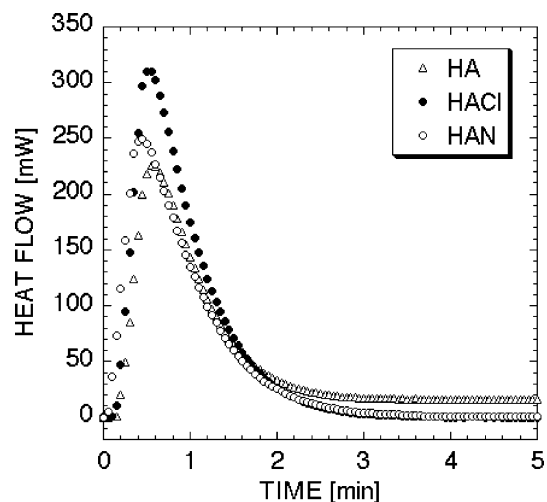


Fig. 3. Reaction heat flow as a function of time caused by  $\text{Mn}^{7+}$ .

Although two exothermic reactions occurred along with a three-electron transfer, the overall heat of the reaction of HAN was greater than that of HACl. Anions had an effect on the redox reactions.

The acidic HACl and HAN showed a higher reactivity than HA. These results can be explained by the fact that the oxidative ability of  $\text{Cr}^{6+}$  is higher in an acidic solution than it is in a basic solution. HA continuously generated heat for more than the maximum test duration, and a violet precipitate was obtained in HA. The origin of the continuous heat generation was unclear; however, a transition among lower oxidation states or the catalytic ability of the surface of the precipitates could be a plausible reason. The overall heat of the reaction of HA exceeded that of HACl and HAN.

## 2.2. Reactions with $\text{Mn}^{7+}$

Fig. 3 shows the heat flow curves of HA, HACl, and HAN caused by  $\text{MnO}_4^-$ . During mixing,  $\text{Mn}^{7+}$  exhibited

a strongly oxidizing character. When the  $\text{MnO}_4^-$  solutions were injected into the substrates, bubbles were produced, and the deep violet color of  $\text{MnO}_4^-$  immediately disappeared. Among the three substrates, only HA gradually produced a white precipitate. The precipitate was considered to be  $\text{Mn}(\text{OH})_2$  [6]. A transition among lower oxidation states or the catalytic ability of the precipitates would provide a plausible explanation, as would  $\text{Cr}^{6+}$ .

HACl and HAN completed the reaction within 30 min, whereas HA continuously generated heat for longer than the maximum test durations. These results are summarized in Table 3. The UV-vis absorptions of manganese in HAG and HAN were too weak for any products to be identified. However,  $[\text{Mn}(\text{H}_2\text{O})_6]^{2+}$  was plausible because of its weak UV-vis absorption and its lowest redox potential among manganese ions.

Although the heat of the reaction was mainly ascribed to  $\text{HONH}_3^+$  in both substrates, the results caused by  $\text{Cr}^{6+}$  and  $\text{Mn}^{7+}$  differed between HACl and HAN.  $\text{Cr}^{6+}$  showed high

Table 2  
Summary of the calorimetric and UV data of the reaction caused by  $\text{Cr}^{6+}$  (calorimetric values are the average of three trials)

Substrate	Maximum heat flow (Mw)	Overall heat of reaction (J)	Distinguishable peaks of UV absorptions (nm)	Color of reaction mixtures or precipitates
HA	137.6	>120	Precipitation	Violet
HACl	234.9	13.5	562.0	Champagne
HAN	280.1	17.1	562.0	Champagne
H <sub>2</sub> O			257.0, 351.0	Yellow

Table 3  
Summary of the calorimetric and UV data of the reaction caused by  $Mn^{7+}$  (calorimetric values are the average of three trials)

Substrate	Maximum heat flow (Mw)	Overall heat of reaction (J)	Distinguishable peaks of UV absorptions (nm)	Color of reaction mixtures or precipitates
HA	224.0	>120	Precipitation	White
HACl	310.0	17.2	Not distinguishable	Colorless
HAN	262.4	16.6	Not distinguishable	Colorless
H <sub>2</sub> O			310.0, 317.0, 507.0, 525.0, 544.5	Deep violet

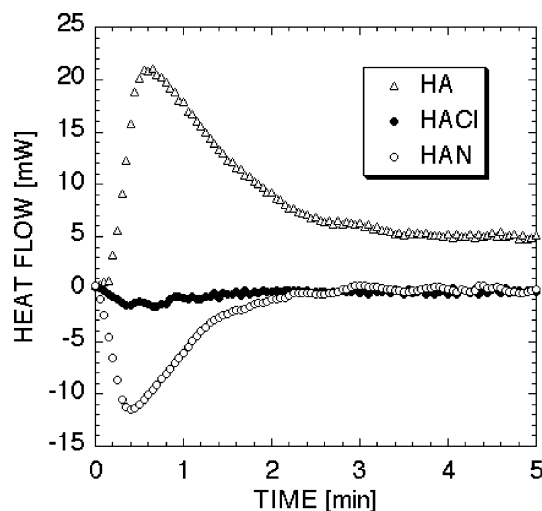


Fig. 4. Reaction heat flow as a function of time caused by  $Co^{2+}$ .

reactivity in HAN, as did  $Mn^{7+}$  in HACl. Anionic effects must exist in the exothermic processes triggered by  $Mn^{7+}$  as well as in those triggered by  $Cr^{6+}$ .

### 2.3. Reactions with $Co^{3+}$ and $Co^{2+}$

Both  $Co^{3+}$  and  $Co^{2+}$  are intermediate oxidation states of cobalt. They may act as either an oxidizer or a reducing agent, depending on the circumstances. The heat flow curves of three substrates caused by  $Co^{2+}$  are shown in Fig. 4. The UV–vis spectra summarized in Table 4 indicated that cobalt, which originated from  $Co(NH_4)_2(SO_4)_2$ , existed as  $[Co(H_2O)_6]^{2+}$  in HACl and HAN. In mixing,  $Co^{2+}$  did not show heat release in HAN or in HACl by considering the heat of dilution. From these results, it can be deduced that no redox reaction occurred in the substances. However,  $Co^{2+}$  continuously generated heat with HA and produced a brown precipitate.

Table 4  
Summary of the calorimetric and UV data of the reaction caused by  $Co^{2+}$  (calorimetric values are the average of three trials)

Substrate	Maximum heat flow (Mw)	Overall heat of reaction (J)	Distinguishable peaks of UV absorptions (nm)	Color of reaction mixtures or precipitates
HA	20.8	>138	Precipitation	Brown
HACl	-1.49	-0.13	510.5	Faint pink
HAN	-11.7	-0.05	509.0	Faint pink
H <sub>2</sub> O			511.5	Faint pink

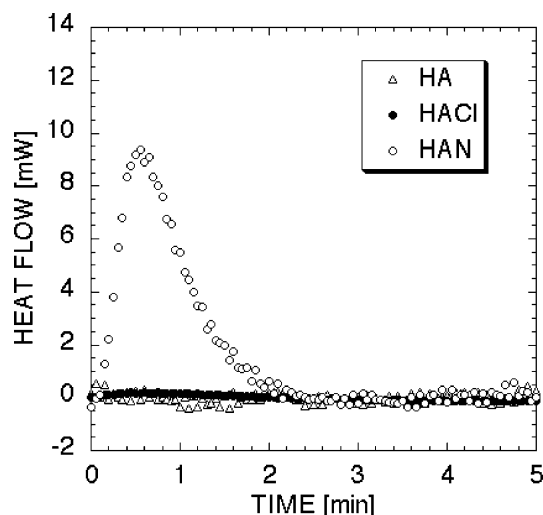


Fig. 5. Reaction heat flow as a function of time caused by  $Co^{3+}$ .

The heat flow curve of three substrates caused by  $Co^{3+}$  is shown in Fig. 5 and calorimetric and UV data are summarized in Table 5. HAN exhibited an exothermic reaction and provided a yellow precipitate in contact with  $Co^{3+}$ . In HACl, neither a peak in the heat flow curve nor evidence of a redox reaction was observed. The orange color of  $[Co(NH_3)_6]^{3+}$  remained in HACl.

Upon mixing with HA, no reaction seemed to occur at the beginning of the monitoring. However, the heat flow curve started to rise gradually following the injection, and it exhibited a peak about 10 h later (Fig. 6). After the induction period, the mixture provided a brown precipitate, although it exhibited no change in color during the early hours.

### 2.4. Reactions with $Cu^{2+}$

Copper has three major oxidation states:  $Cu^{2+}$ ,  $Cu^+$ , and  $Cu^0$ . Since,  $Cu^{2+}$  is the highest oxidation state,  $Cu^{2+}$  is liable to undergo reduction despite its low oxidation number.

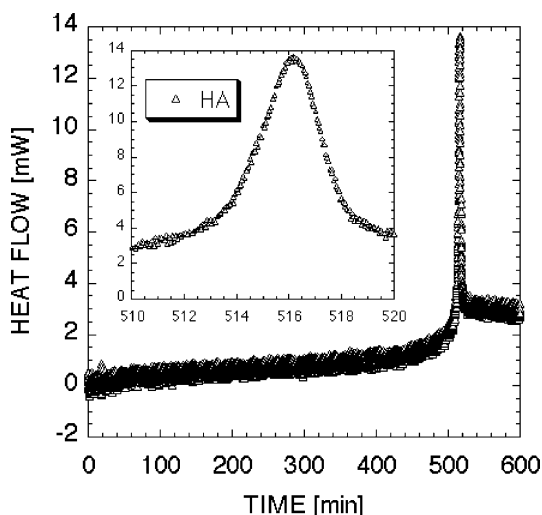


Fig. 6. Exothermic behavior of HA after an induction period caused by  $\text{Co}^{2+}$ .

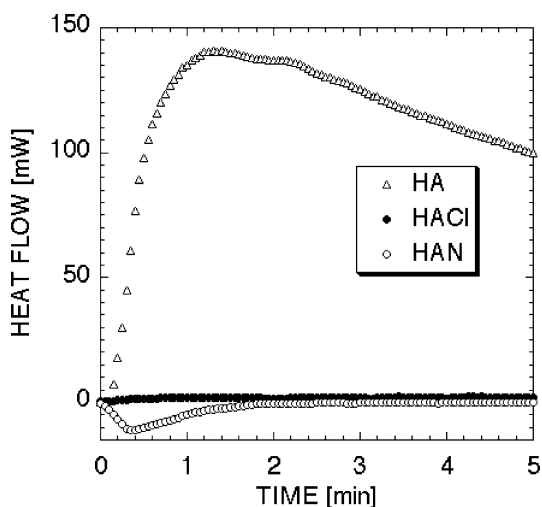


Fig. 7. Reaction heat flow as a function of time caused by  $\text{Cu}^{2+}$ .

The heat flow curve caused by  $\text{Cu}^{2+}$  is shown in Fig. 7. Table 6 is a summary of the experimental results. The blue color of  $[\text{Cu}(\text{H}_2\text{O})_6]^{2+}$ , which originated from  $\text{Cu}(\text{NH}_4)_2(\text{SO}_4)$ , was too faint to clearly indicate whether the reactions occurred in HAcI and HAN. In HA, a yellow green film, which later changed to brown, was observed on the liquid surface.

No distinguishable absorption peak was observed in the UV–vis spectra, even in a mixture of  $\text{Cu}(\text{NH}_4)_2(\text{SO}_4)$  and

Table 6  
Summary of the calorimetric data of the reaction caused by  $\text{Cu}^{2+}$

Substrate	Maximum heat flow (Mw)	Overall heat of reaction (J)	Color of reaction mixtures or precipitates
HA	136.6	>92.9	Yellow green
HAcI	2.70	>49.9	Faint blue
HAN	-11.2	-0.16	Faint blue
$\text{H}_2\text{O}$			Faint blue

Table 7

Comparison of the overall heat of reaction caused by transition metals and the results from DSC measurements. All values are the amount of heat released as 1g of 50%HA

Mixed metal or cell of DSC	Overall heat of reaction (J/g, 50% HA)
$\text{Cr}^{3+}$ : $\text{Cr}(\text{NH}_3)(\text{SO}_4)_2$	19
$\text{Cr}^{6+}$ : $\text{K}_2\text{Cr}_2\text{O}_7$	908
$\text{Mn}^{7+}$ : $\text{KMnO}_7$	908
$\text{Co}^{2+}$ : $\text{Co}(\text{NH}_4)(\text{SO}_4)_2$	737
$\text{Co}^{3+}$ : $[\text{Co}(\text{NH}_3)_6]\text{Cl}_3$	1045
$\text{Cu}^{2+}$ : $\text{Cu}(\text{NH}_4)(\text{SO}_4)_2$	703
Stainless cell	1960 [8]
Glass capillary	2250 [8]

$\text{H}_2\text{O}$ . This result for  $\text{Cu}(\text{NH}_4)_2(\text{SO}_4)$  was supported by previously collected data indicating that absorption peaks of  $[\text{Cu}(\text{H}_2\text{O})_6]^{2+}$ , which were not covered by UV–vis spectroscopy, appeared at 1,060, 765, and 200 nm [7].

As another plausible product,  $[\text{Cu}(\text{NH}_3)_4]^{2+}$ , which has an absorption peak at 590 nm, was not detected, whereas the APTAC experiments showed the complex from 50%HA and copper [2]. In order to generate  $[\text{Cu}(\text{NH}_3)_4]^{2+}$ , ammonia-rich conditions are required, and the mild condition used in this experiment did not allow this complex to be generated. The appearance of a red precipitate suggested that  $\text{Cu}_2\text{O}$  had formed.

In addition to the spectroscopic results, calorimetric experiments showed the exothermic behavior of HA and HAcI. Both substrates continuously generated a heat flow. The maximum heat flow of HA was not high; however, a continuous release of heat resulted in high overall heat of the reaction. As for HAN, the heat of absorption was observed in the experiments. The amount of heat absorbed was corrected by the heat of dilution and reduced to almost zero.

## 2.5. Comparison with DSC

Table 7 summarizes the results so that the heat releases by DSC can be compared with those of SuperCRC of 50%HA

Table 5  
Summary of the calorimetric and UV data of the reaction caused by  $\text{Co}^{2+}$  (calorimetric values are the average of three trials)

Substrate	Maximum heat flow (Mw)	heat of reaction (J)	Distinguishable peaks of UV absorptions (nm)	Color of reaction mixtures or precipitates
HA	12.2	>97.4	Precipitation	Brown
HAcI	–	–	339.5, 474.0	Orange
HAN	9.1	1.28	Precipitation	Yellow
$\text{H}_2\text{O}$			340.0, 474.0	Orange

The results by SuperCRC were converted to heat per gram of 50% HA.

The heat of the reaction by SuperCRC was less than one half of that by DSC. However, the results suggested that HA would have been capable of releasing heat since a continuous heat release was not achieved during the maximum test durations. These results indicate that it must be hazardous for HA to be in contact with metals regardless of the room temperature, particularly if the contact is of long duration.

### 3. Conclusion

The thermal behaviors of HA, HAC1, and HAN under redox reaction conditions were investigated using a small-scale reaction calorimeter, SuperCRC, and UV–vis spectroscopy. The reactions were triggered by aqueous solutions of transition metals:  $\text{Cr}^{3+}$ ,  $\text{Cr}^{6+}$ ,  $\text{Mn}^{7+}$ ,  $\text{Co}^{3+}$ ,  $\text{Co}^{2+}$ , and  $\text{Cu}^{2+}$ .

All exothermic reactions were accompanied by precipitation or a change in the UV–vis spectra. The UV–vis spectra suggested that the transition metals, such as  $\text{Cr}^{6+}$  and  $\text{Mn}^{7+}$ , were reduced in HAC1 and HAN. HA provided precipitation upon contact with all metals. All metals, except  $\text{Cr}^{3+}$ , continuously reacted with HA. An induction period was observed for HA with  $\text{Co}^{3+}$ .

Continuous heat release might cause an explosion if the heat accumulates, especially, on a large scale. Safe handling

requires that the transition of metal impurities be prevented when HA is treated.

### Acknowledgements

The authors are grateful to Hosoya Pyrotechnics Co. Ltd., Japan, for providing HAN.

### References

- [1] L.O. Cisneros, W.J. Rogers, M.S. Mannan, Adiabatic calorimetric decomposition studies of 50 wt.% hydroxylamine/water, *J. Hazard. Mater.* A82 (2001) 13–24.
- [2] L.O. Cisneros, W.J. Rogers, M.S. Mannan, Effect of air in the thermal decomposition of 50 mass% hydroxylamine/water, *J. Hazard. Mater.* A95 (2002) 13–25.
- [3] Y. Iwata, H. Koseki, Risk evaluation of decomposition of hydroxylamine/water solution at various concentrations, *Process Saf. Prog.* 21 (2) (2002) 136–141.
- [4] M. Tamura, An explosion accident of hydroxylamine, *J. Jpn. Soc. Saf. Eng* 40 (5) (2001) 321–327 (in Japanese).
- [5] M. Kumasaki, Y. Fujimoto, T. Ando, Calorimetric behaviors of hydroxylamine and its salts caused by Fe(III), *J. Loss Prevent. Process Ind.* 16 (2003) 507–512.
- [6] Bailar et al. editors. *Comprehensive Inorganic Chemistry*. vol. 3 Pergamon Press; 1973.
- [7] The Chemical Society of Japan, *Handbook of Chemistry: Pure Chemistry II*. 3rd ed. Tokyo: Maruzen; 1993 (in Japanese).
- [8] National Institute of Industrial Safety. *Safety Guide of the National Institute of Industrial Safety*. NIIS-SG-No. 1: Tokyo; 2003 (in Japanese).